Article

Optical Properties and Aggregation of Phenothiazine-based Dye Sensitisers for Solar Cells Applications: A Combined Experimental and Computational Investigation

Saurabh Agrawal, Mariachiara Pastore, Gabriele Marotta, Marri Anil Reddy, Malapaka Chandrasekharam, and Filippo De Angelis

Just Accepted

Optical Properties and Aggregation of Phenothiazine-based Dye-Sensitisers for Solar Cells Applications: A Combined Experimental and Computational Investigation

Saurabh Agrawal,[a] Mariachiara Pastore,[a] Gabriele Marotta,[a] Marri Anil Reddy,[b]

Malapaka Chandrasekharam,[b], Filippo De Angelis[a],**

[a] Computational Laboratory for Hybrid/Organic Photovoltaics (CLHYO), CNR-ISTM

Perugia, Via elce di Sotto 8, I-06213, Perugia, Italy.

[b] Indian Institute of Chemical Technology, Hyderabad, India.

Corresponding author E-mail: chandra@iict.res.in. Tel: 04027193186.

Corresponding author E-mail: filippo@thch.unipg.it. Tel: +39 075-5855523. Fax: +39

075-5855606

RECEIVED DATE (to be automatically inserted after your manuscript is accepted if required according to the journal that you are submitting your paper to)

Abstract

Combining computational modeling and experimental optical analyses, we investigate two prototypical phenothiazine-based organic solar cells sensitizers with the aim to understand the individual effects of solvation and aggregation on the dyes optical properties. Dye solvation and aggregation play a crucial role in determining the photo-electrochemical properties of these systems and the interplay of these two factors can lead to a misinterpretation of the underlying phenomenology due to their similar spectroscopic signals. In particular, upon adsorption of the dye onto the metal oxide surface, the dye UV-vis absorption spectrum may attain either a blue or a red shift compared to the dye in solution, which can either be originated from aggregation of surface-adsorbed dye and/or solvatochromism in the initial dye solution. Understanding the origin of these spectral changes along with their possible effect on charge-transfer properties is important for the further improvement of Dye-sensitized Solar Cells. Based on our results, we show that the optical properties of phenothiazine-based dyes are much more sensitive to the type of explicit interactions with the solvent than to aggregation on the TiO_2 surface. Therefore, this study gets important new insights into the understanding of these properties and may assist the molecular engineering of new and more efficient dyes sensitizers.

2

1. Introduction

Dye-sensitized solar cells (DSCs),[1] since its first successful demonstration by O'Regan and Grätzel in 1991,[2] have gained considerable attention as a viable alternative to conventional photovoltaics for the direct conversion of light into electrical energy at low cost and with high efficiency. In these photovoltaic devices charge generation takes place by photo-excitation of dye molecules adsorbed onto a wide band gap metal oxide surface, such as TiO_2. Upon light irradiation, the dye injects a photo-excited electron into the semiconductor conduction band (CB), which is transported to the transparent conducting oxide (typically FTO), to reach the external circuit. In most typical applications, a redox shuttle (I^-/I_3^- or Co(II)/Co(III)) in a liquid electrolyte solution reduces the oxidized dye and gets reduced again by receiving charge back from counter electrode connected with the external circuit.

Among the basic DSCs components, i.e. the dye, the metal oxide and the redox shuttle, the chemical nature and structure of the dye is by far the most investigated subject, with the ultimate aim of increasing the dye molar extinction coefficient and shifting the dye absorption towards the near-IR region, thus enhancing the overlap between the solar emission and the dye absorption spectrum and eventually achieving higher DSCs photocurrents. Traditionally, the most commonly employed dyes in DSCs are Ruthenium(II) polypyridyl complexes.[1] [3, 4] Recently, Zn(II)-porphyrins have shown high efficiency when coupled to Co(II)/Co(III) redox shuttles, exceeding 12%.[5] Fully organic dyes have also attracted considerable interest, [1, 6] due to their higher synthetic flexibility, scalability and lower environmental impact; in conjunction with transition metal-based electrolytes, organic dyes have been shown to clearly outperform Ru(II)-based dyes.[7-11] A typical push-pull organic

3

dye consists of an electron donating group, a linker group and an electron accepting/anchoring group. A large number of organic dyes have been reported with different types of donors, linkers and acceptors. Among the donor moieties, N,N-dimethylaniline group,[12, 13] coumarins,[14-20] tetrahydoquinolines,[21, 22] pyrrolidine,[23] carbazoles,[24] diphenylamine,[25] triphenylamine, [6, 26-28] etc., have been widely employed. On the other side, basically three types of acceptor/anchor groups, namely cyanoacrylic acid, [6, 12-29] carboxylic acid [30-32] and rhodanine-3-acetic acid[33, 34 35] are widely used in organic dyes sensitizers. Due to continuous development of new dyes, it is a challenge to summarize a complete list here. To get an idea of the varieties of dyes being developed, the reader is referred to the recent reviews by Mishra et al.[36] and Hagfeldt et al.[1]

Electrostatic and non-covalent interactions of the dye with the polar surface and adjacent dye molecules may lead to the formation of an ordered assembly of dye aggregates on titania.[37-41] Dye aggregation is known be the Achille's heel of most of organic sensitizers, usually leading to intermolecular excited state quenching, and hence reducing the DSCs photocurrent and overall power output.[20, 37, 42] The formation of stable aggregates on the TiO_2 surface is usually manifested by a considerable broadening and blue or red shift, depending on whether H-[43, 44] or J-type [45] of aggregates are formed, of the UV-vis absorption spectrum upon TiO_2 adsorption compared to that for of dyes in solution.[34, 46] In some selected cases, a controlled aggregation has proven to enhance the photocurrent generation due to the larger light-absorption window of the aggregates, possibly combined to an efficient charge transfer from the aggregate excited state to the semiconductor. [38, 42, 47, 48] The use of anti-aggregation coadsorbents,[49-51 52, 53] among which the most widely employed is

4

chenodeoxycholic acid (CDCA), [52-54] has been reported to effectively suppress dye aggregation on the TiO_2 surface, yielding to notably improved cell performances for dye being critically affected by aggregation. Since CDCA competes with the dye for TiO_2 absorption, thus breaking undesired dye/dye intermolecular interactions, a general decrease of the dye loading is also typically observed with a consequent decrease of the light harvesting efficiency of the photoelectrode, which is however usually offset by an improved charge generation efficiency due to suppression of intermolecular excited state quenching and filtering effects.

Successful theoretical and computational modeling of dye/dye intermolecular interactions at the dye-sensitized TiO_2 heterointerface[46, 55] and of the associated spectroscopic phenomena[56] has been recently reported by some of us, highlighting the subtle relations existing between the dye molecular structure and its tendency to form dense packing on the semiconductor surface. Exploiting the experience in the computational modeling of organic-dye-sensitized TiO_2 interfaces, here we report a joint experimental and computational investigation aimed to investigate the optical properties in relation to the possible formation of interfacial aggregates of phenothiazine (PTZ) based dyes, such as **CS1A** in Figure 1, which was previously reported by Yang et al. and coded as Pt-C6.[57] The PTZ core, by virtue of its high absorption extinction coefficient and strong electron-donating capabilities, has been widely employed in the design of both fully organic (as electron donor[29, 58-65] and as conjugated linker[54, 57, 66]) and ruthenium sensitizers.[67]

5
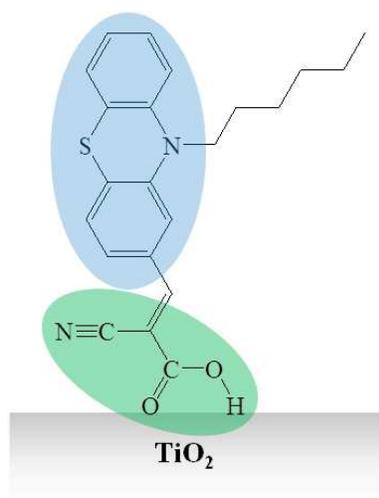
Figure 1. Molecular structure of the CS1A sensitizer.

The CS1A dye features a -C_6H_{13} alkyl chain, linked to the nitrogen atom of the PTZ unit, which may possibly modulate the dye-aggregation upon adsorption on the TiO$_2$ surface. Notably, aggregation phenomena should also be attenuated by the non-planar "butterfly" conformation of the PTZ unit. The synthesis and photovoltaic characterization of the same dye, coded PtC6, has been previously reported by Yang et al.,[57] and related PTZ-based dyes with different alkyl chains have also been widely investigated, namely a C_4H_9, [29] an 2-ethyl-hexyl chain (C_2H_5-C_6H_{12}) [59] and a C_2H_5 [68] chains, with the corresponding dyes coded T2-1, PR6C1 and SB respectively. Contrasting optical properties for PTZ-based dyes in solution and upon adsorption on TiO$_2$ have been reported, with sizable solvatochromic shifts reported from THF to CH$_2$Cl$_2$ solutions and moderate to strong blue shifts being observed upon dye adsorption on TiO$_2$, see below.

Understanding the structural and electronic properties of the dye-sensitized interface from an atomistic computational modeling perspective is a pre-requisite for

6

the subsequent molecular engineering of new dyes with improved characteristics, thus,

here we have systematically studied the effect of the CS1A dye protonation,

solvatochromism and dye binding to TiO_2, including aggregation, on the optical

properties of this system. By combining basic UV-vis spectroscopic investigations

with DFT/TDDFT calculations we show that the optical properties of phenothiazine-

based dyes are much more sensitive to the type of explicit interactions with the

solvent than to aggregation on the TiO_2 surface.

2. Experimental and Computational Details

2.1 Synthetic procedure.

The synthesis of the CS1A dye is described in Scheme 1. Commercially available

phenothiazine was subjected to N-alkylation using bromohexane followed by

Vilsmeier-Haack formylation. The resulting 10-hexyl-10H-phenothiazine-3-

carbaldehyde underwent smooth Knoevenagel condensation with cyanoacetic acid to

afford CS1A in 75% yield.

Scheme 1: Synthesis of CS1A
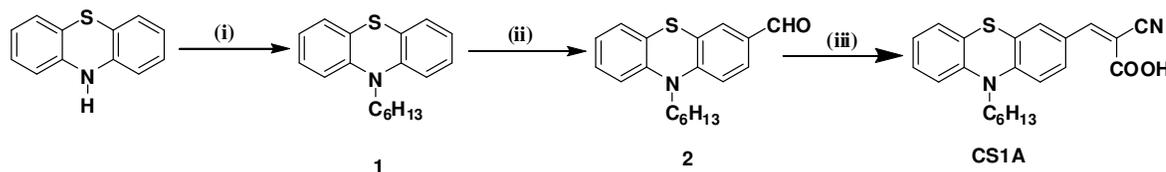
Reagents & conditions: (i) NaH, DMF, 1-dibromohexane, RT, overnight (ii) DMF,

$POCl_3$, 1,2-dichloroethane, reflux overnight (iii) Piperidine, $CHCl_3$, cyano aceticacid,

reflux, 8hrs.

7

The synthetic route of compounds 1 and 2 is reported in Supporting Information, along with the NMR spectra of compounds 1, 2 and CS1A, Figures S1, S2 and S3 respectively. For the synthesis of CS1A, compound 2 (130 mg, 0.466 mmol) in $CHCl_3$ (8 mL) and 2-cyanoacetic acid (99 mg, 1.165 mmol) were refluxed for 8 h in the presence of piperidine (0.151 mL, 1.538 mmol). After cooling to room temperature, 5 mL of 2 M aqueous HCl was added and the mixture was stirred for 30 min. Then the mixture was washed with water and extracted three times with chloroform. The combined organic fractions were washed with brine and dried over Na_2SO_4. The solvent was removed under reduced pressure and the residue was purified by column chromatography using methanol/dichloromethane (1/9; v/v) as eluent to give dark red powder **CS1A** (75%).

2.2 Preparation of the TiO_2 substrate

Fluorine-doped tin oxide coated (FTO) glass electrode (Nippon Sheet Glass Co., Japan) with a sheet resistance of 8–10 ohm m^{-2} and an optical transmission of >80% in the visible range was used. Anatase TiO_2 colloids (particle size ~13 nm) were obtained from commercial sources (Ti-Nanoxide D/SP, Solaronix). The nanocrystalline TiO_2 thin films of approximately 20 μm thickness were deposited onto the conducting glass by screen-printing. The film was then sintered at 500 ^{0}C for 1 h. The film thickness was measured with a Surfcom 1400A surface profiler (Tokyo Seimitsu Co. Ltd). The electrodes were impregnated with a 50 mM titanium tetrachloride solution and sintered at 500 ^{0}C. The dye solutions (2 × 10−4 M) were prepared in 1:1 acetonitrile and *tert*-butyl alcohol solvents. The electrodes were immersed in the dye solutions and then kept at 25 °C for 20 h to adsorb the dye onto the TiO_2 surface.

8

2.3 Computational Details

We modeled both the real CS1A / PtC6 (-C_6H_{13} chain) dyes and the T2-1 dye (-C_4H_9 chain). This allows us to gain insight into the impact of the alkyl chain length in affecting the aggregation pattern. A neutral, stoichiometric $(TiO_2)_{38}$ cluster exposing anatase (101) surface was used as our TiO_2 model.[69, 70] It was recently shown that TiO_2 anatase slabs of thickness similar to our cluster nicely reproduce the electronic structure of thicker films.[71, 72] We carried out geometry optimization of the stand-alone dyes and dyes@$(TiO_2)_{38}$ using the B3LYP hybrid functional and a standard 6-31G* basis sets. Solvent effects were added using the polarizable continuum model of solvation (C-PCM)[73] as implemented in the Gaussian 09 code.[74] Geometry optimizations were followed by excited state TDDFT calculations to simulate the UV-vis spectra of the dyes in solution and of the surface adsorbed dyes and their aggregates. The spectral profiles have been obtained by gaussian convolutions with FWHM=0.37 eV.

To model the dye aggregation pattern, we choose four possible positions (P) for adsorption of dye on TiO_2 nanoparticle (Figure 2). Here, positions P2 and P3 are used to model weakly interacting aggregates (a0), positions 1 (P1) and 2 (P2) are utilized to model aggregate 1 (a1), positions 2 (P2) and 3 (P3) are used for aggregate 2 (a2). Aggregate formation with position 1 and position 4 is structurally hindered due to presence of butyl chain. Here, the butyl chain of dye adsorbed at P4 clashes with the dye adsorbed at P1.
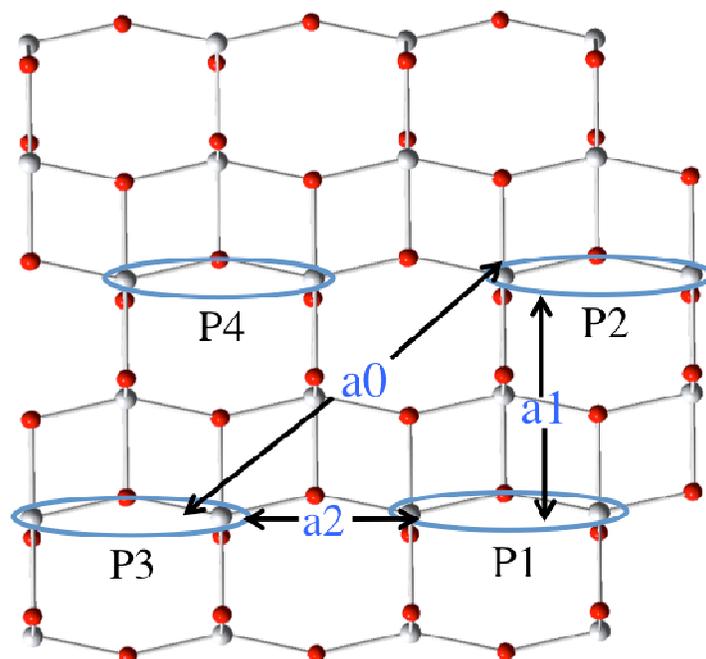
Figure 2. Aggregation scheme for the T2-1 dimeric configurations adsorbed on the (TiO$_2$)$_{38}$. Here, a0 involves positions (P2 and P3), a1 involves positions P1 and P2 and a2 involves positions (P1 and P3).

Following a previous study from some of us,[46] we calculate the interaction energies for the surface adsorbed dyes by MP2 calculations, both in vacuum and in solution, at the geometries of the protonated and deprotonated dyes adsorbed on TiO$_2$.

3. Results and Discussion

3.1 Experimental optical properties

A large body of data have been reported in previous studies concerning the variation of the PTZ-dyes optical properties in solution and when adsorbed on TiO$_2$, which we collect in Table 1. The experimental UV-vis absorption spectrum of CS1A, here recorded in tetrahydrofuran (THF) solution, presents two bands, centered at 438 (2.83) and 316 (3.92) nm (eV) as displayed in Figure 3. When changing the solvent

10

from THF to dichloromethane (DCM), the main absorption peak shifts to 463 nm

(2.68 eV). Our data is perfectly consistent with previously reported data for Pt-C6[57] in

THF (438 nm, Table 1) and for PR6C1[59] in DCM (462 nm, Table 1). The sizable

solvatochromic shift (0.15 eV) observed from THF to DCM solution is quite

surprising, especially considering that the two solvents have a similar dielectric

constant (7.43 and 8.93, respectively).

Upon adsorption of CS1A onto TiO_2, the main visible absorption band appears

slightly broadened and red-shifted, with an absorption maximum at 442 (2.80) nm

(eV). Our result is in good agreement with the reported absorption maximum

measured for the PR6C1[59] and T2-1[29] dyes on TiO_2 (433 and 425 nm, respectively)

but differs significantly from the data reported for Pt-C6[57] (392 nm). Our data is also

very similar to what reported for the triphenyl-amine-substituted PTZ dyes of Ref.

[66], dyes coded P1-P3, for which a slight red shift and broadening of the optical

absorption spectrum was reported upon dye adsorption on TiO_2.
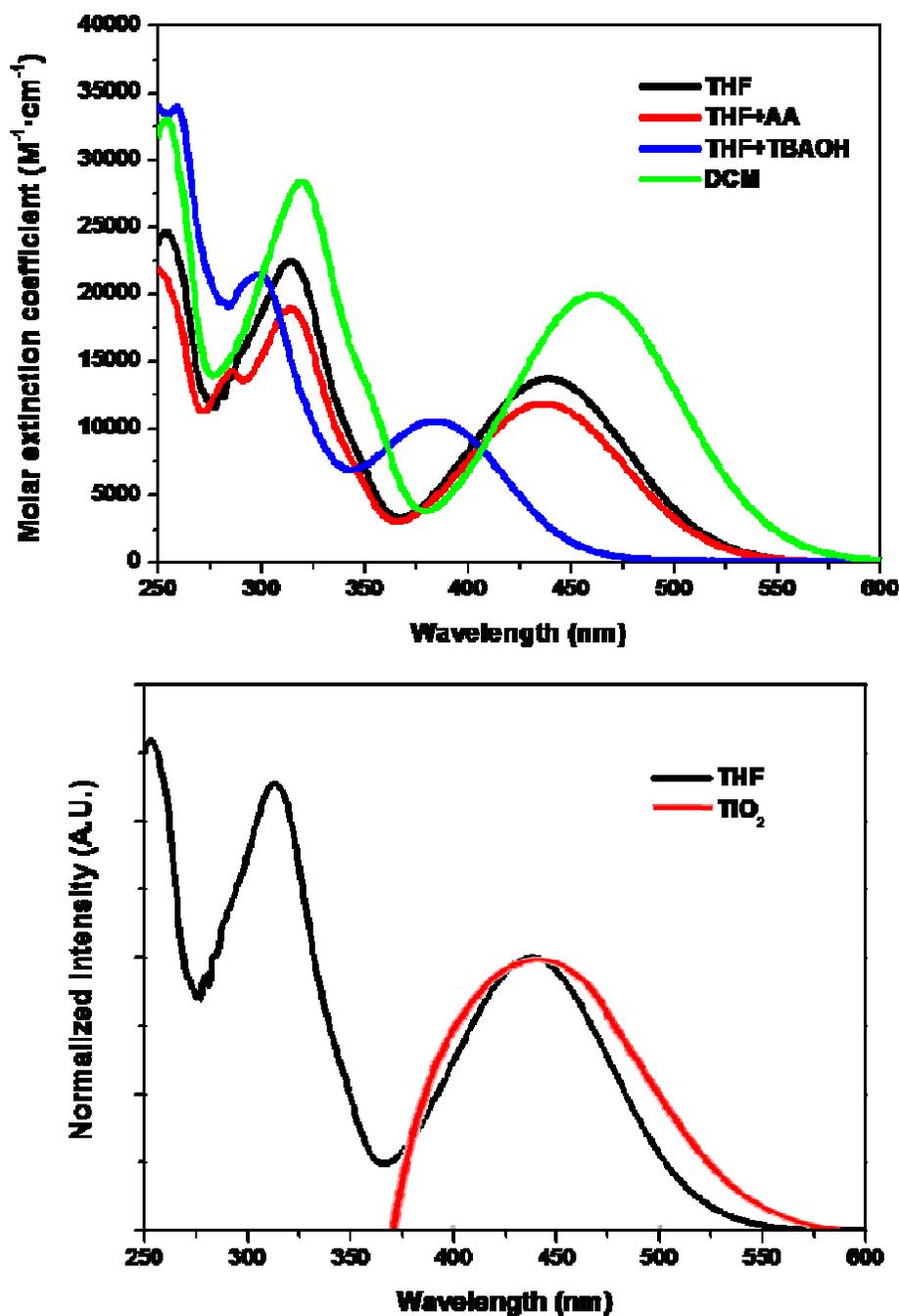
Figure 3. Top: Absorption spectra of CS1A dye in DCM solution (green line) and in THF solution (black), with the addition of acetic acid (AA, red line) and with the addition of TBAOH (blue line). Bottom: Normalized absorption spectra in THF (black line) and on TiO_2 film (red line).

12

Table 1. Survey of the experimental UV-vis absorption maxima of PTZ-dyes in solution and on TiO_2.

Dye code	Alkyl chain	λ_{max} (sol.)	λ_{max} (TiO_2)
SB[68]	C2	439 (THF)	---
T2-1[29]	C4	452 (CH_2Cl_2)	425
Pt-C6[57]	C6	438 (THF)	392
CS1A[a]	C6	463 (CH_2Cl_2)	442
		438 (THF)	
		438 (THF+AA)	
		384 (THF+TBAOH)	
PR6C1[59]	C2-C6	462 (CH_2Cl_2)	433

[a] this work

Assuming, that the nature and length of the alkyl chain does not influence the dye electronic structure, the data in THF are consistently blue-shifted compared to data in dichloromethane, with our data aligning on this trend. Second, both blue and red-shifts can be observed upon dye adsorption onto TiO_2. These shifts are usually interpreted in terms of the type of aggregates formed on the surface, although it has to be stressed that with such a solvent-induced variability on the dye optical properties it is quite difficult on the basis of this data alone, i.e. of the shift in optical properties from solution to surface adsorbed dyes, to provide a clear insight into the aggregation of this type of dyes on titania. As a matter of fact, the solvent induced shifts can be

13

most likely related to the acid/base chemistry of the cyanoacrylic group, with deprotonation (occurring in certain solvents) leading to sizable blue-shifted absorption spectra,[75-77] while in absence of aggregation phenomena the optical properties of dyes on TiO_2 are somehow intermediate between those of the protonated and deprotonated dyes in solution. [76] This picture is corroborated by the observed strong blue-shift (0.41 eV) which is measured for the CS1A dye upon addition of the TBAOH base to the dye THF solution, shifting the absorption from 438 to 384 nm, Table 1. Notably, addition of acetic acid (AA) to the dye solution in THF does not lead to any sizable shift, suggesting that the dye is protonated in this solvent.

3.2 Computational analyses

3.2.1 Dyes in solution

To provide a rationale for the observed experimental picture, we have first performed DFT/TDDFT calculations for the isolated dye in solution. In Figure 4 we report the optimized geometry of the CS1A dye, which shows the expected non-planar butterfly conformation, along with isodensity plots of the dye HOMO and LUMO.

14
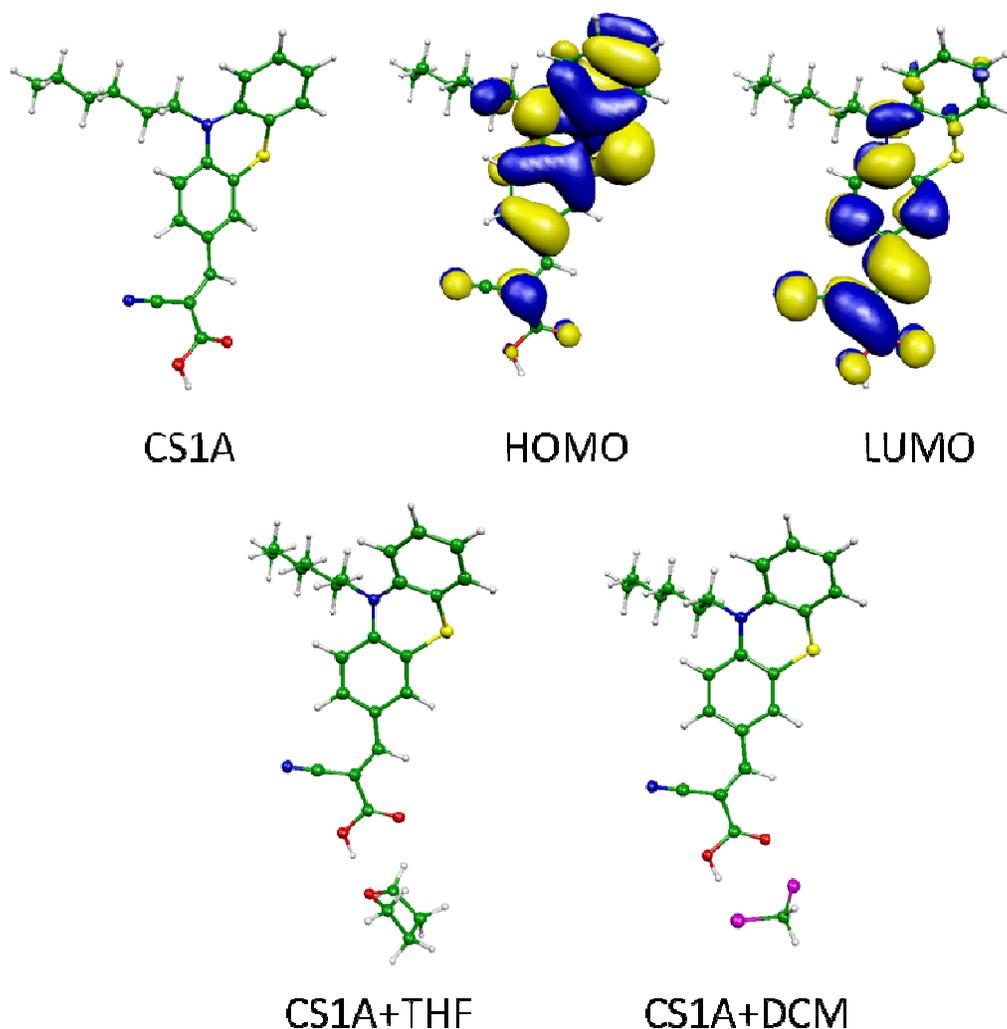
Figure 4. Optimized geometries of CS1A, CS1A+ a THF molecules and CS1A+ a DCM molecule. Also shown are isodensity plots of the HOMO and LUMO molecular orbitals.

To check the effect of different solvents as well as of acid-base chemistry on the dyes optical properties, we performed a series of calculations in different solvents, including one explicit solvent molecule, Figure 4, for the protonated and deprotonated dyes, as summarized in Table 2. From now on we report data in eV, which is a more useful scale for comparative purposes.

15

Table 2. TDDFT-calculated lowest transition energies (eV) for the CS1A dye in THF and DCM solutions, for the protonated and deprotonated dyes (1st and 2nd column). The 3rd and 4th columns report results for the protonated dye interacting with an explicit solvent molecule (either THF or DCM).

	Solvent					
	THF		DCM		THF+1THF	DCM+1DCM
	Prot.	Deprot.	Prot.	Deprot.	Prot.	Prot.
$S_0 \rightarrow S_1$	2.56 (0.33)	2.96 (0.00)	2.55 (0.34)	2.99 (0.00)	2.63 (0.35)	2.53 (0.35)
$S_0 \rightarrow S_2$	3.45 (0.34)	3.16 (0.31)	3.45 (0.34)	3.15 (0.32)	3.53 (0.34)	3.43 (0.35)
$S_0 \rightarrow S_3$	3.98 (0.20)	3.24 (0.02)	3.99 (0.20)	3.27 (0.01)	4.01 (0.22)	3.98 (0.22)

The protonated CS1A features a single $S_0 \rightarrow S_1$ transition of HOMO$\rightarrow$LUMO character, Figure 4, which is responsible of the main visible dye absorption. The HOMO shows a delocalized charge density over the entire dye with higher localization on the donor moiety. In the same way, the LUMO is also delocalized over

16

the entire dye with higher localization on the acceptor moiety. Greater localization of HOMO on donor and LUMO on anchor moieties is desirable to realize an efficient charge separation leading to push-pull effect. The $S_0 \rightarrow S_1$ transition is calculated at 2.56 and 2.55 eV in THF and DCM, respectively. It is clear how the simple use of a continuum solvation model provides very similar optical properties for this system, as expected on the basis of the similar dielectric constant of THF and DCM, missing the above-mentioned 0.15 solvatochromic shift. For the deprotonated dye the $S_0 \rightarrow S_1$ transition (2.96/2.99 eV) has zero oscillator strength, followed at higher energy by an intense $S_0 \rightarrow S_2$ transition, which we calculate at 3.16 and 3.15 eV in THF and DCM, respectively. The strong blue shift of the absorption maximum, which nicely parallels the measured spectral shifts, stems from the strong LUMO destabilization which is only partly offset by the HOMO destabilization, as is typically observed for cyanoacrylic-based dyes.[76]

The calculated data for the protonated dye are slightly red-shifted (0.13 eV) compared to the experimental absorption maximum in DCM (2.68 eV), possibly due the dependence of B3LYP on 0.2 R^{-1} instead of exact R^{-1} (R is the charge separation distance).[76, 78] We also repeated TDDFT calculations in DCM using the CAM-B3LYP functional,[79] to check whether improved results could be obtained. Our data showed intense $S_0 \rightarrow S_1$ transitions of 3.19 and 3.72 eV for the protonated and deprotonated dye, respectively, which are notably blue-shifted compared to the experimental absorption maxima. Thus, keeping in mind the 0.13 eV shift of the calculated absorption spectra compared to experimental data, the B3LYP functional seems to provide results in closer agreement with the experiment. The effect of the exchange-correlation functional was also checked for dyes on TiO_2, see below.

17

To check the effect of explicit solvation on the calculated optical properties, we considered a THF and a DCM molecule binding the dye carboxylic group, bottom of Figure 4, optimizing the dye/solvent geometries in the respective continuum solvent. The idea is that hydrogen bonding to the THF oxygen and possibly to the DCM chloride could lead to some shift in the optical properties, analogously to what is observed upon dye deprotonation. Our results show indeed a sizable interaction between the protonated carboxylic group and the THF oxygen, as signaled by a hydrogen-bond distance of 1.67 Å. As expected, a rather weak interaction is calculated between the carboxylic group and the DCM solvent, with a H-Cl distance of 2.47 Å. The explicit dye/solvent interactions translate into a sizable blue-shift (0.07 eV) of the main visible absorption band for the dye+THF system, compared to the isolated dye in THF solution, while the dye+DCM systems shows a modest red-shift (0.02 eV). On overall our data including explicit solvation show a solvatochromic blue-shift of 0.10 eV going from THF to DCM, which nicely compares with the experimentally observed 0.15 eV shift.

3.2.2 Dyes on TiO$_2$

We now move on to describe the properties of the TiO$_2$-adsorbed dye. Here for simplicity we initially simulated the adsorption of the CS1A dye with a C4-alkyl chain (i.e. the T2-1 dye), moving to the real CS1A dye in the second stage of the calculations. To study the surface-adsorbed dye@TiO$_2$ complexes, we considered the dye to be adsorbed in a dissociative bridged bidentate mode, Figure 5. Kalyanasundaram and Grätzel[80] have discussed several adsorption mode of carboxylic acid anchor on titania surface. Recently, FT-IR experiments and computational investigations[12, 19, 81-89] have indeed suggested that both acetic and cyanoacrylic acid

18

1
2
3   groups anchor on the TiO$_2$ surface through bidentate carboxylate anchoring.
4
5
6
7
8
9
10
11
12
13
14
15
16
17
18
19
20
21
22
23
24
25
26
27
28
29
30
31
32
33
34
35
36
37
38
39
40
41
42
43
44
45
46
47
48
49
50
51
52
53
54
55
56
57
58   19
59
60

1
2
3
4
5
6
7
8
9
10
11
12
13
14
15
16
17
18
19
20
21
22
23
24
25
26
27
28
29
30
31
32
33
34
35
36
37
38
39
40
41
42
43
44
45
46
47
48
49
50
51
52
53
54
55
56
57
58
59
60
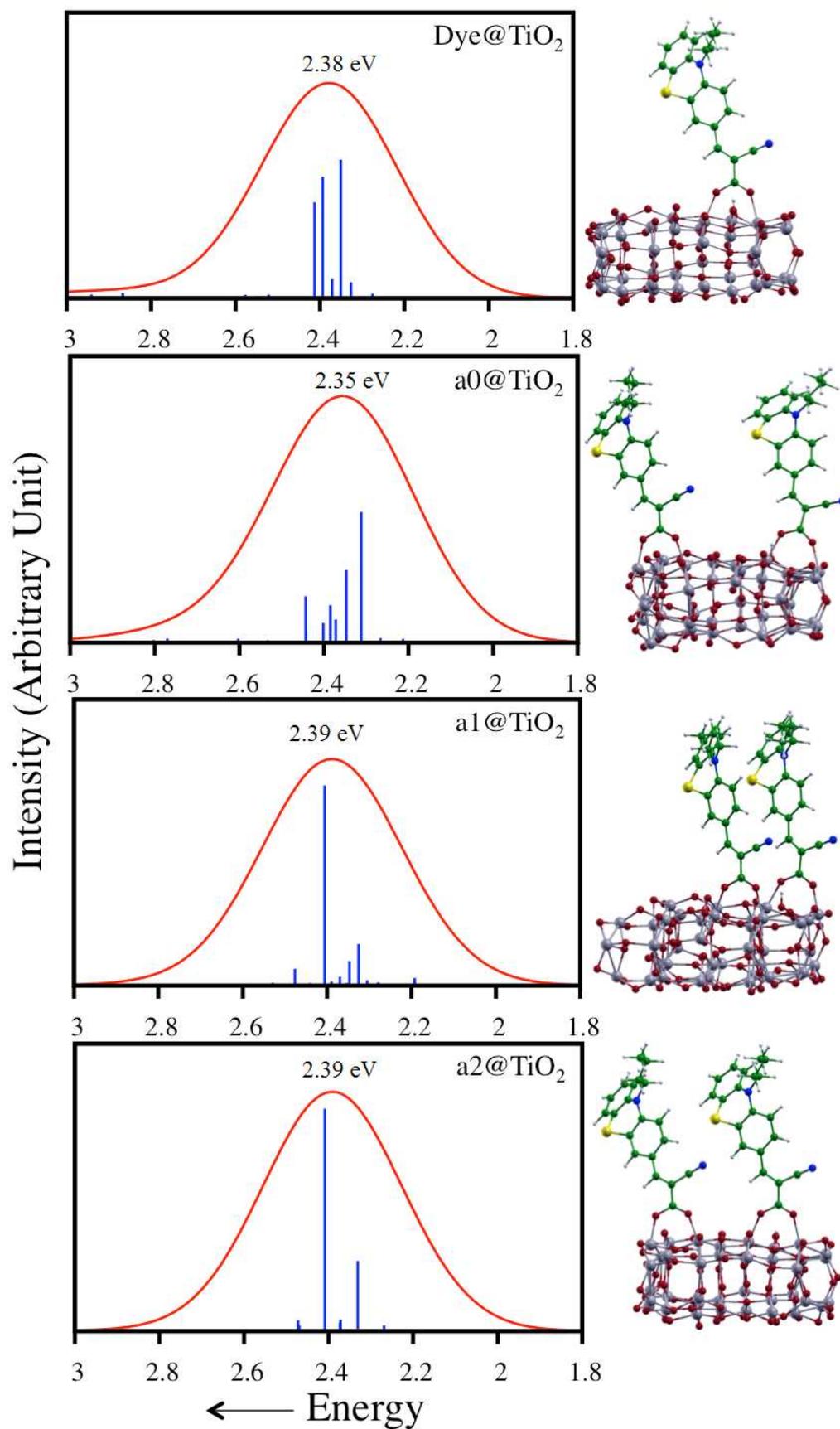
Figure 5. Left: Calculated absorption spectra (eV) of the single dye on TiO_2, and of the a0, a1 and a2 aggregates on TiO_2, along with calculated absorption maxima. Right: Optimized structures of the corresponding systems.

By looking at the alignment of the dye MOs with the semiconductor energy levels, Figure 6, we observe that the HOMO (found at -5.49 eV), lies, as expected, within the HOMO-LUMO gap of the TiO_2 nanoparticle, whereas the dye LUMO (-2.59 eV) lies far above the TiO_2 conduction band bottom. This alignment of MOs suggests that the excitation of dye should results in efficient electron transfer to conduction band of TiO_2 nanoparticle. The isolated TiO_2 nanoparticle gives first excitation at 3.79 eV, which is in agreement with the experimental values for TiO_2 nanoparticle of a few nanometer size.[90, 91] Upon adsorption on TiO_2, the dye LUMO partly mixes with TiO_2 unoccupied states, leading to a broadening of the isolated dye LUMO. The electronic structure of the various aggregates is rather similar to that of the TiO_2-adsorbed single dye, apart from the slight splitting of the HOMOs due to the presence of the aggregates.

21
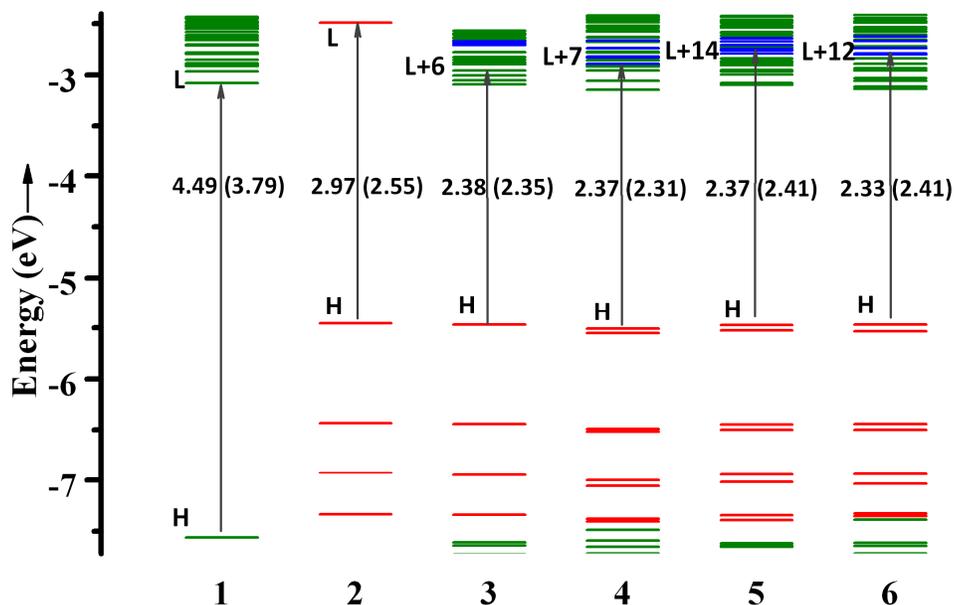
Figure 6. Molecular orbital energy level diagram of isolated $(TiO_2)_{38}$ nanoparticle (1), isolated dye (2), dye@TiO$_2$ complex (3), a0@TiO$_2$ aggregate (4), a1@TiO$_2$ aggregate (5) and a2@TiO$_2$ aggregate (6). Here, red represents localization of MOs on the dye, green represents MO localization on the nanoparticle and blue MO localized on both dye and nanoparticle. The values within parenthesis are the TDDFT excitation energies corresponding to the lowest intense transitions, see Table S1 of Supporting Information. For TiO$_2$ the indicated excitation refers to the lowest excited state.

The B3LYP/TDDFT calculated UV-vis spectrum for the single dye on TiO$_2$, surrounded by the DCM solvent, shows an absorption maximum at 2.38 eV, see Figure 5. This data is red-shifted by 0.17 eV compared to the calculated absorption maximum for the isolated dye in DCM solution (2.55 eV). The observed red-shift is possibly due to the artificial lowering of the dye@TiO$_2$ excited states due to the increased charge-transfer characterizing the surface-adsorbed dye,[75] although a slight modulation of the absorption properties due to the interaction of the deprotonated dye

22

carboxylic group with the undercoordinated surface Ti(IV) ions is also likely to occur. To check the effect of the increased charge-transfer due to the dye/semiconductor interaction we performed CAM-B3LYP/TDDFT calculations on the single dye on TiO_2 in DCM solution, maintaining the same optimized geometry, finding a lowest and intense excitation energy at 3.10 eV, i.e. 0.09 eV red-shifted compared to the isolated dye in solution. Notice that, as previously found,[75] the alignment of dye/semiconductor excited states is not correctly reproduced by CAM-B3LYP, which positions the intense dye→dye excited state about 1 eV below the lowest dye→semiconductor excitation. It is in any case interesting to notice that, despite the strong overestimate of the excitation energies for both the isolated and surface-adsorbed dye by CAM-B3LYP, the slightly reduced red-shift observed upon dye adsorption with this functional (0.09 eV) compared to B3LYP (0.17 eV) is possibly related to an improved description of the excited states for the surface-adsorbed dye compared to the dye in solution, which are characterized by an increased degree of charge-transfer. Taken together, our results indicate that a red-shift of the optical absorption spectrum accompanies the dye interaction with the semiconductor.

Considering the somehow problematic description of dye/semiconductor excited state alignment found by CAM-B3LYP, and the similar behavior upon dye adsorption on TiO_2, results obtained by the B3LYP functional are mainly discussed here. The calculated absorption spectrum consists of several photo-excitations, Figure 5. A few of these excitations showing comparable oscillator strengths along with their contributing molecular orbitals (MOs) are tabulated in Table S1 of Supporting Information. All these excitations are originated from the HOMO, lying at a similar energy to that of isolated dye, Figure 6, and mainly localized on the dye. Among the

23

several unoccupied orbitals involved in these excitations, the LUMO+6, LUMO+7 and LUMO+9, localized both on the TiO$_2$ substrate and the dye, show major contributions to the optical absorption.

Moving to the dimeric aggregates, whose optimized structures are also reported in Figure 5, our calculated structures show that the a0 aggregate is characterized by two weakly interacting dyes; the a1 aggregate shows the two dyes to form a slipped stack; while the a2 aggregate shows the two dye molecules to adsorb in a sidewise pattern, see Figure 5. The stability of the dimeric dye aggregates for the deprotonated dyes suggests that the three investigated structures (a0, a1 and a2) have rather similar interaction energies, see Table 3. We also notice that the length of the alkyl chain (C4 or C6) does not lead to sizable changes in the energetics of the dimer interaction energies.

Table 3. Interaction binding energies (kcal/mol) for the dimeric aggregates referred the isolated dye for the deprotonated and protonated systems in vacuo and in DCM solution.

Configuration	Binding Energies (kcal/mol)			
	C4 (T2-1)	C6 (CS1A)		
	0H/solv	0H/solv	1H/solv	1H/vac[a]
a0	-3.4	-3.5	+0.3	+0.2
a1	-2.1	-1.4	+4.9	+4.3
a2	-1.0	-1.0	+4.8	+5.5

[a] data *in vacuo* are calculated on the geometries optimized in DCM.

As expected, the interaction energies for the deprotonated dyes are lower (even repulsive) than those for the protonated dyes. For the protonated a1 and a2 aggregates we calculate a dimer formation energy of 4.9 and 4.8 kcal/mol in DCM solution, which for a2 (a1) increases (decreases) to 5.5 (4.3) kcal/mol in vacuo. On overall this

24

data suggests that formation of dye aggregates on the TiO_2 surface is moderately energetically accessible. We remark indeed that for the indoline D102 dye, which is prone to form surface-adsorbed dye aggregates, we calculated MP2 binding energies for the most stable protonated dimer in vacuo of ~14 kcal/mol, with a value of ~9 kcal/mol for the deprotonated species in solution.[92]

Regarding the optical absorption properties of the dye aggregates, we notice that the calculated UV-vis spectra of the a0 system shows an absorption maximum at 2.35 eV, i.e. only 0.03 eV red-shifted compared to that of a single dye on TiO_2, Figure 5, in line with the weak aggregate interaction characterizing this system. The UV-vis spectrum calculated for the a0 dimer by CAM-B3LYP shows an absorption maximum at 3.07 eV, i.e. only 0.03 eV red-shifted compared to that calculated for a single adsorbed dye (3.10 eV), essentially confirming the trend outlined by the B3LYP data. For the a1 and a2 aggregates the B3LYP-calculated spectra show absorption maxima at 2.39 eV, Figure 5, essentially coinciding with that of the isolated dye on TiO_2. On overall our data suggest that the investigated class of dyes has a moderate tendency to form aggregates on TiO_2, with an associated optical response which, under our experimental conditions, is quite similar to that of the protonated dyes in solution. This picture is also in line with the non-beneficial effect of the CDCA co-adsorbent when used in conjunction with PTZ-based dyes,[57, 68] which essentially diminished the dye loading without improving any photovoltaic parameter, [68] clearly signaling weakly aggregation dependent photovoltaic properties for these dyes.

4. Conclusions

This study reports and compares the outcomes of solvation and aggregation of two phenothiazine derived dyes, namely the CS1A/Pt-C6 (-C_6H_{13} chain) dyes and the T2-

25

1 dye (-C$_4$H$_9$ chain), combining basic optical characterization with DFT/TDDFT calculations. A variety of different optical data has been reported for PTZ-based dyes, including a strong solvatochromism moving from THF to DCM, and small or strong blue shifts upon dye adsorption on TiO$_2$. Such spectral shifts can either be originated from aggregation of surface-adsorbed dye and/or solvatochromism in the initial dye solution. Understanding the origin of these spectral changes along with their possible effect on charge-transfer properties is important for the further improvement of dye-sensitized solar cells, allowing the design of new and more efficient dyes, which mimise the use of anti-aggregant co-adsorbents.

To understand the origin of the experimental phenomenology, we utilized different solvation models, including explicit solvation, as well as aggregation models for the surface adsorbed dyes. Our results suggest that solvation plays a major role in determining the optical properties of this class of organic dyes, with the solvatochromism observed moving from THF to DCM (0.15 eV red-shift) being reproduced only upon describing the explicit solute-solvent interactions characterizing the two types of solvents. Furthermore this study shows that dye aggregation on the TiO$_2$ surface does not sizably affect the spectral properties of these dyes (<0.03 blue or red-shifts) and is only moderately energetically favorable, with the length of the dye alkyl chain (C4 or C6) not affecting the calculated energetics. To quantify the propensity of PTZ-based dyes to form aggregates on titania we compared the calculated aggregate stability for the CS1A dye (5.5 kcal/mol) with previously reported data for the indoline D102 dye (14 kcal/mol), which is prone to form stable aggregates on the TiO$_2$ surface, as revealed by the strong red-shift and broadening of the optical absorption spectrum measured for this system. Our data thus confirm the

26

small propensity of PTZ-based dyes to form aggregates on the TiO_2 surface, which

also explains the non-beneficial effect of the CDCA co-adsorbent in DSCs employing

this class of dyes. On overall, our study has revealed important new insights into the

understanding of dye aggregation on the TiO_2 surface, which may assist the molecular

engineering of new and more efficient dyes sensitizers and a deeper comprehension of

the dye-sensitized heterointerface.

Acknowledgements

Supporting Information Available. Synthetic details and NMR spectra. Excited

state composition and optimized structures. This material is available free of charge

via the Internet at http://pubs.acs.org .

References

(1)   Hagfeldt, A.; Peter, L., *Dye-sensitized Solar Cells* EPFL Press: Lausanne, 2010; p 323-403.
(2)   O'Regan, B.; Grätzel, M. A Low-Cost, High-Efficiency Solar Cell Based on Dye-Sensitized Colloidal TiO_2 Films. *Nature* **1991,** *353*, 737-740.
(3)   Nazeeruddin, M. K.; De Angelis, F.; Fantacci, S.; Selloni, A.; Viscardi, G.; Liska, P.; Ito, S.; Takeru, B.; Grätzel, M. Combined Experimental and DFT-TDDFT Computational Study of Photoelectrochemical Cell Ruthenium Sensitizers. *J. Am. Chem Soc.* **2005,** *127*, 16835-16847.
(4)   Grätzel, M. Conversion of Sunlight to Electric Power by Nanocrystalline Dye-Sensitized Solar Cells. *J. Photochem. Photobiol. A* **2004,** *164*, 3-14.
(5)   Yella, A.; Lee, H.-W.; Tsao, H. N.; Yi, C.; Chandiran, A. K.; Nazeeruddin, M. K.; Diau, E. W.-G.; Yeh, C.-Y.; Zakeeruddin, S. M.; Grätzel, M. Porphyrin-Sensitized Solar Cells with Cobalt (II/III) Based Redox Electrolyte Exceed 12 Percent Efficiency. *Science* **2011,** *334*, 629-634.
(6)   Hagberg, D. P.; Marinado, T.; Karlsson, K. M.; Nonomura, K.; Qin, P.; Boschloo, G.; Brinck, T.; Hagfeldt, A.; Sun, L. Tuning the HOMO and LUMO Energy Levels of Organic Chromophores for Dye Sensitized Solar Cells. *J. Org. Chem.* **2007,** *72*, 9550-9556.

(7)   Daeneke, T.; Kwon, T.-H.; Holmes, A. B.; Duffy, N. W.; Bach, U.; Spiccia, L. High-Efficiency Dye-Sensitized Solar Cells with Ferrocene-based Electrolytes. *Nat. Chem.* **2011,** *3*, 213-217.

(8)   Feldt, S. M.; Gibson, E. A.; Gabrielsson, E.; Sun, L.; Boschloo, G.; Hagfeldt, A. Design of Organic Dyes and Cobalt Polypyridine Redox Mediators for High-Efficiency Dye-Sensitized Solar Cells. *J. Am. Chem Soc.* **2010,** *132*, 16714-16724.

(9)   Feldt, S. M.; Cappel, U. B.; Johansson, E. M. J.; Boschloo, G.; Hagfeldt, A. Characterization of Surface Passivation by Poly(methylsiloxane) for Dye-Sensitized Solar Cells Employing the Ferrocene Redox Couple. *J. Phys. Chem. C* **2010,** *114*, 10551-10558.

(10)   Bai, Y.; Zhang, J.; Zhou, D.; Wang, Y.; Zhang, M.; Wang, P. Engineering Organic Sensitizers for Iodine-Free Dye-Sensitized Solar Cells: Red-Shifted Current Response Concomitant with Attenuated Charge Recombination. *J. Am. Chem Soc.* **2011,** *133*, 11442-11445.

(11)   Cameron, P. J.; Peter, L. M.; Zakeeruddin, S. M.; Grätzel, M. Electrochemical Studies of the $Co(III)/Co(II)(dbbip)_2$ Redox Couple as a Mediator for Dye-Sensitized Nanocrystalline Solar Cells. *Coord. Chem. Rev.* **2004,** *248*, 1447-1453.

(12)   Hara, K.; Sato, T.; Katoh, R.; Furube, A.; Yoshihara, T.; Murai, M.; Kurashige, M.; Ito, S.; Shinpo, A.; Suga, S. Novel Conjugated Organic Dyes for Efficient Dye‐Sensitized Solar Cells. *Advanced Functional Materials* **2005,** *15*, 246-252.

(13)   Hara, K.; Kurashige, M.; Ito, S.; Shinpo, A.; Suga, S.; Sayama, K.; Arakawa, H. Novel Polyene Dyes for Highly Efficient Dye-Sensitized Solar Cells. *Chem. Comm.* **2003**, 252-253.

(14)   Hara, K.; Kurashige, M.; Dan-oh, Y.; Kasada, C.; Shinpo, A.; Suga, S.; Sayama, K.; Arakawa, K. Design of New Coumarin Dyes Having Thiophene Moieties for Highly Efficient Organic-Dye-Sensitized Solar Cells. *New. J. Chem.* **2003,** *27*, 783-785.

(15)   Hara, K.; Sayama, K.; Ohga, Y.; Shinpo, A.; Suga, S.; Arakawa, H. A Coumarin-Derivative Dye Sensitized Nanocrystalline TiO_2 Solar Cell Having a High Solar-Energy Conversion Efficiency up to 5.6%. *Chem. Comm.* **2001,** *0*, 569-570.

(16)   Hara, K.; Tachibana, Y.; Ohga, Y.; Shinpo, A.; Suga, S.; Sayama, K.; Sugihara, H.; Arakawa, H. Dye-sensitized Nanocrystalline TiO_2 Solar Cells Based on Novel Coumarin Dyes. *Sol. Eergy. Mater. Sol. Cells* **2003,** *77*, 89-103.

(17)   Hara, K.; Wang, Z.-S.; Sato, T.; Furube, A.; Katoh, R.; Sugihara, H.; Dan-oh, Y.; Kasada, C.; Shinpo, A.; Suga, S. Oligothiophene-Containing Coumarin Dyes for Efficient Dye-Sensitized Solar Cells. *J. Phys. Chem. B* **2005**, 15476-15482.

(18)   Hara, K.; Miyamoto, K.; Abe, Y.; Yanagida, M. Electron Transport in Coumarin-Dye-Sensitized Nanocrystalline TiO_2 Electrodes. *J. Phys. Chem. B,* **2005,** *109*, 23776-23778.

(19)   Hara, K.; Sato, T.; Katoh, R.; Furube, A.; Ohga, Y.; Shinpo, A.; Suga, S.; Sayama, K.; Sugihara, H.; Arakawa, H. Molecular Design of Coumarin Dyes for Efficient Dye-Sensitized Solar Cells. *J. Phys. Chem. B* **2003,** *107*, 597-606.

(20)   Wang, Z.-S.; Cui, Y.; Dan-oh, Y.; Kasada, C.; Shinpo, A.; Hara, K. Thiophene-Functionalized Coumarin Dye for Efficient Dye-Sensitized Solar Cells: Electron Lifetime Improved by Coadsorption of Deoxycholic Acid. *J. Phys. Chem. C* **2007,** *111*, 7224-7230.

(21)   Chen, R.; Yang, X.; Tian, H.; Sun, L. Tetrahydroquinoline Dyes With Different Spacers for Organic Dye-Sensitized Solar Cells. *J. Photochem. Photobiol. A: Chemistry* **2007,** *189*, 295-300.

(22)   Chen, R.; Yang, X.; Tian, H.; Wang, X.; Hagfeldt, A.; Sun, L. Effect of Tetrahydroquinoline Dyes Structure on the Performance of Organic Dye-Sensitized Solar Cells. *Chem. Mater.* **2007,** *19*, 4007-4015.

(23)   Campbell, W. M.; Jolley, K. W.; Wagner, P.; Wagner, K.; Walsh, P. J.; Gordon, K. C.; Schmidt-Mende, L.; Nazeeruddin, M. K.; Wang, Q.; Grätzel, M.*, et al.* Highly Efficient Porphyrin Sensitizers for Dye-Sensitized Solar Cells. *J. Phys. Chem. C* **2007,** *111*, 11760-11762.

28

(24)   Wang, Z. S.; Cui, Y.; Dan-Oh, Y.; Kasada, C.; Shinpo, A.; Hara, K. Molecular Design of Coumarin Dyes for Stable and Efficient Organic Dye-Sensitized Solar Cells. *J. Phys. Chem. C* **2008,** *112*, 17011-17017.

(25)   Thomas, K. R. J.; Lin, J. T.; Hsu, Y.-C.; Ho, K.-C. Organic Dyes Containing Thienylfluorene Conjugation for Solar Cells. *Chem. Comm.* **2005,** *0*, 4098-4100.

(26)   Hwang, S.; Lee, J. H.; Park, C.; Lee, H.; Kim, C.; Park, C.; Lee, M. H.; Lee, W.; Park, J.; Kim, K.*, et al.* A Highly Efficient Organic Sensitizer for Dye-Sensitized Solar Cells. *Chem. Comm.* **2007**, 4887-4889.

(27)   Xu, W.; Peng, B.; Chen, J.; Liang, M.; Cai, F. New Triphenylamine-Based Dyes for Dye-Sensitized Solar Cells. *J. Phys. Chem. C* **2008,** *112*, 874-880.

(28)   Liu, W. H.; Wu, I. C.; Lai, C. H.; Lai, C. H.; Chou, P. T.; Li, Y. T.; Chen, C. L.; Hsu, Y. Y.; Chi, Y. Simple Organic Molecules Bearing a 3,4-ethylenedioxythiophene Linker for Efficient Dye-Sensitized Solar Cells. *Chem. Comm.* **2008**, 5152-5154.

(29)   Tian, H.; Yang, X.; Chen, R.; Pan, Y.; Li, L.; Hagfeldt, A.; Sun, L. Phenothiazine Derivatives for Efficient Organic Dye-Sensitized Solar Cells. *Chem. Comm.* **2007,** *0*, 3741-3743.

(30)   Tan, S.; Zhai, J.; Fang, H.; Jiu, T.; Ge, J.; Li, Y.; Jiang, L.; Zhu, D. Novel Carboxylated Oligothiophenes as Sensitizers in Photoelectric Conversion Systems. *Chem. Europ. J.* **2005,** *11*, 6272-6276.

(31)   Tanaka, K.; Takimiya, K.; Otsubo, T.; Kawabuchi, K.; Kajihara, S.; Harima, Y. Development and Photovoltaic Performance of Oligothiophene-sensitized TiO_2 Solar Cells. *Chem. Lett.* **2006,** *35*, 592-593.

(32)   Yum, J.; Walter, P.; Huber, S.; Rentsch, D.; Geiger, T.; Nuesch, F.; De Angelis, F.; Grätzel, M.; Nazeeruddin, M. K. Efficient Far Red Sensitization of Nanocrystalline TiO_2 Films by an Unsymmetrical Squaraine Dye. *J Am Chem Soc* **2007,** *129*, 10320-10321.

(33)   Schmidt-Mende, L.; Bach, U.; Humphry-Baker, R.; Horiuchi, T.; Miura, H.; Ito, S.; Uchida, S.; Grätzel, M. Organic Dye for Highly Efficient Solid-State Dye-Sensitized Solar Cells. *Adv. Mater.* **2005,** *17*, 813-815.

(34)   Horiuchi, T.; Miura, H.; Uchida, S. Highly-Efficient Metal-Free Organic Dyes for Dye-Sensitized Solar Cells. *Chem. Comm.* **2003**, 3036–3037.

(35)   Horiuchi, T.; Miura, H.; Sumioka, K.; Uchida, S. High Efficiency of Dye-Sensitized Solar Cells Based on Metal-Free Indoline Dyes. *J. Am. Chem Soc.* **2004,** *126*, 12218-12219.

(36)   Mishra, A.; Fischer, M.; Bäuerle, P. Metal-Free Organic Dyes for Dye-Sensitized Solar Cells: From Structure: Property Relationships to Design Rules. *Angew. Chem. Int. Ed.* **2009,** *48*, 2474-2499.

(37)   Tatay, S.; Haque, S. A.; O'Regan, B.; Durrant, J. R.; Verhees, W. J. H.; Kroon, J. M.; Vidal-Ferran, A.; Gavina, P.; Palomares, E. Kinetic Competition in Liquid Electrolyte and Solid-State Cyanine Dye Sensitized Solar Cells. *J. Mater. Chem.* **2007,** *17*, 3037-3044.

(38)   Sayama, K.; Tsukagoshi, S.; Hara, K.; Ohga, Y.; Shinpou, A.; Abe, Y.; Suga, S.; Arakawa, H. Photoelectrochemical Properties of J Aggregates of Benzothiazole Merocyanine Dyes on a Nanostructured TiO_2 Film. *J. Phys. Chem. B* **2002,** *106*, 1363-1371.

(39)   Burfeindt, B.; Hannappel, T.; Storck, W.; Willig, F. Measurement of Temperature-Independent Femtosecond Interfacial Electron Transfer from an Anchored Molecular Electron Donor to a Semiconductor as Acceptor. *J. Phys. Chem.* **1996,** *100*, 16463-16465.

(40)   Liu, D.; Fessenden, R. W.; Hug, G. L.; Kamat, P. V. Dye Capped Semiconductor Nanoclusters. Role of Back Electron Transfer in the Photosensitization of SnO_2 Nanocrystallites with Cresyl Violet Aggregates. *J. Phys. Chem. B* **1997,** *101*, 2583-2590.

(41)   Tian, H.; Yang, X.; Chen, R.; Zhang, R.; Hagfeldt, A.; Sun, L. Effect of Different Dye Baths and Dye-Structures on the Performance of Dye-Sensitized Solar Cells Based on Triphenylamine Dyes. *J. Phys. Chem. C* **2008,** *112*, 11023–11033.

(42)   Ehret, A.; Stuhl, L.; Spitler, M. T. Spectral Sensitization of TiO_2 Nanocrystalline Electrodes with Aggregated Cyanine Dyes. *J. Phys. Chem. B* **2001,** *105*, 9960-9965.

(43)   Bujdák, J.; Iyi, N. Molecular Orientation of Rhodamine Dyes on Surfaces of Layered Silicates. *The Journal of Physical Chemistry B* **2005,** *109*, 4608-4615.

29

(44)   Mulhern, K. R.; Orchard, A.; Watson, D. F.; Detty, M. R. Influence of Surface-Attachment Functionality on the Aggregation, Persistence, and Electron-Transfer Reactivity of Chalcogenorhodamine Dyes on TiO2. *Langmuir* **2012,** *28*, 7071-7082.

(45)   Würthner, F.; Kaiser, T. E.; Saha-Möller, C. R. J-Aggregates: From Serendipitous Discovery to Supramolecular Engineering of Functional Dye Materials. *Angew. Chem. Int. Ed.* **2011,** *50*, 3376-3410.

(46)   Pastore, M.; De Angelis, F. Aggregation of Organic Dyes on TiO$_2$ in Dye-Sensitized Solar Cells Models: An ab Initio Investigation. *ACS nano* **2010,** *4*, 556-562.

(47)   Kawasaki, M.; Aoyama, S. High Efficiency Photocurrent Generation by Two-Dimensional Mixed J-aggregates of Cyanine Dyes. *Chem. Comm.* **2004**, 988-989.

(48)   Khazraji, A. C.; Hotchandani, S.; Das, S.; Kamat, P. V. Controlling Dye (Merocyanine-540) Aggregation on Nanostructured TiO$_2$ Films. An Organized Assembly Approach for Enhancing the Efficiency of Photosensitization. *J. Phys. Chem. B* **1999,** *103*, 4693-4700.

(49)   Wang, P.; Zakeeruddin, S. M.; Comte, P.; Charvet, R.; Humphry-Baker, R.; Grätzel, M. Enhance the Performance of Dye-Sensitized Solar Cells by Co-grafting Amphiphilic Sensitizer and Hexadecylmalonic Acid on TiO$_2$ Nanocrystals. *J. Phys. Chem. B* **2003,** *107*, 14336–14341.

(50)   Wang, M.; Li, X.; Lin, H.; Peter Pechy; Zakeeruddin, S. M.; Grätzel, M. Passivation of Nanocrystalline TiO$_2$ Junctions by Surface Adsorbed Phosphinate Amphiphiles Enhances the Photovoltaic Performance of Dye Sensitized Solar Cells. *Dalton Trans.* **2009,** *45*, 10015–10020.

(51)   Han, L.; Islam, A.; Chen, H.; Malapaka, C.; Chiranjeevi, B.; Zhang, S.; Yang, X.; Yanagida, M. High-Efficiency Dye-Sensitized Solar Cell with a Novel Co-Adsorbent. *Energy Environ. Sci.* **2012,** *5*, 6057-6060.

(52)   Wang , Q.; Campbell, W. M.; Bonfantani, E. E.; Jolley, K. W.; Officer, D. L.; Walsh, P. J.; Gordon, K. C.; Humphry-Baker, R.; Nazeeruddin, M. K.; Grätzel, M. Efficient Light Harvesting by Using Green Zn-Porphyrin-Sensitized Nanocrystalline TiO$_2$ Films. *J. Phys Chem. B* **2005,** *109*, 15397–15409.

(53)   Lee, C.-W.; Lu, H.-P.; Lan, C.-M.; Huang, Y.-L.; Liang, Y.-R.; Yen, W.-N.; Liu, Y.-C.; Lin, Y.-S.; Diau, E. W.-G.; Yeh, C.-Y. Novel Zinc Porphyrin Sensitizers for Dye-Sensitized Solar Cells: Synthesis and Spectral, Electrochemical, and Photovoltaic Properties. *Chem. Eur. J.* **2009,** *15*, 1403-1412.

(54)   Li, J.; Wu, W.; Yang, J.; Tang, J.; Long, Y.; Hua, J. Effect of Chenodeoxycholic Acid (CDCA) Additive on Phenothiazine Dyes Sensitized Photovoltaic Performance. *Sci. China Chem.* **2011,** *54*, 699-706.

(55)   Planells, M.; Pellejà, L.; Clifford, J. N.; Pastore, M.; De Angelis, F.; López, N.; Marder, S. R.; Palomares, E. Energy Levels, Charge Injection, Charge recombination and Dye Regeneration Dynamics for Donor−Acceptor π-Conjugated Organic Dyes in Mesoscopic TiO$_2$ Sensitized Solar Cells. *Energy Environ. Sci.* **2011,** *4*, 1820-1829.

(56)   Pastore, M.; De Angelis, F. Computational Modeling of Stark Effects in Organic Dye-Sensitized TiO$_2$ Heterointerfaces. *J. Phys. Chem. Lett.* **2011,** *2*, 1261-1267.

(57)   Yang, C.-J.; Chang, Y. J.; Watanabe, M.; Hon, Y.-S.; Chow, T. J. Phenothiazine Derivatives as Organic Sensitizers for Highly Efficient Dye-Sensitized Solar Cells. *J. Mater. Chem.* **2012,** *22*, 4040-4049.

(58)   Marszalek, M.; Nagane, S.; Ichake, A.; Humphry-Baker, R.; Paul, V.; Zakeeruddin, S. M.; Grätzell, M. Tuning Spectral Properties of Phenothiazine Based Donor- pi-Acceptor Dyes for Efficient Dye-Sensitized Solar Cells. *Journal of Materials Chemistry* **2012,** *22*, 889-894.

(59)   Park, S. S.; Won, Y. S.; Choi, Y. C.; Kim, J. H. Molecular Design of Organic Dyes with Double Electron Acceptor for Dye-Sensitized Solar Cell. *Energy & Fuels* **2009,** *23*, 3732-3736.

(60)   Meyer, T.; Ogermann, D.; Pankrath, A.; Kleinermanns, K.; Müller, T. J. J. Phenothiazinyl Rhodanylidene Merocyanines for Dye-Sensitized Solar Cells. *The Journal of Organic Chemistry* **2012,** *77*, 3704-3715.

30

(61)   Tsao, M.-H.; Wu, T.-Y.; Wang, H.-P.; Sun, I. W.; Su, S.-G.; Lin, Y.-C.; Chang, C.-W. An Efficient Metal-Free Sensitizer for Dye-Sensitized Solar cells. *Mater. Lett.* **2011,** *65*, 583-586.

(62)   Tian, H.; Yang, X.; Chen, R.; Hagfeldt, A.; Sun, L. A Metal-Free "black dye" for Panchromatic Dye-Sensitized Solar Cells. *Energy Environ. Sci.* **2009,** *2*, 674-677.

(63)   Xie, Z.; Midya, A.; Loh, K. P.; Adams, S.; Blackwood, D. J.; Wang, J.; Zhang, X.; Chen, Z. Highly Efficient Dye-Sensitized Solar Cells Using Phenothiazine Derivative organic dyes. *Progr. Photovoltaics* **2010,** *18*, 573-581.

(64)   Kim, S. H.; Kim, H. W.; Sakong, C.; Namgoong, J.; Park, S. W.; Ko, M. J.; Lee, C. H.; Lee, W. I.; Kim, J. P. Effect of Five-Membered Heteroaromatic Linkers to the Performance of Phenothiazine-Based Dye-Sensitized Solar Cells. *Org. Lett.* **2011,** *13*, 5784-5787.

(65)   Wan, Z.; Jia, C.; Duan, Y.; Zhou, L.; Lin, Y.; Shi, Y. Phenothiazine-triphenylamine Based Organic Dyes Containing Various Conjugated Linkers for Efficient Dye-Sensitized Solar Cells. *J. Mater. Chem.* **2012,** *22*, 25140-25147.

(66)   Wu, W.; Yang, J.; Hua, J.; Tang, J.; Zhang, L.; Long, Y.; Tian, H. Efficient and Stable Dye-Sensitized Solar Cells Based on Phenothiazine Sensitizers With Thiophene Units. *J. Mater. Chem.* **2010,** *20*, 1772-1779.

(67)   Yin, J.-F.; Chen, J.-G.; Lin, J.-T. s.; Bhattacharya, D.; Hsu, Y.-C.; Lin, H.-C.; Ho, K.-C.; Lu, K.-L. Enhanced Light-Harvesting Capability by Phenothiazine in Ruthenium Sensitizers With Superior Photovoltaic Performance. *J. Mater. Chem.* **2012,** *22*, 130-139.

(68)   Cao, D.; Peng, J.; Hong, Y.; Fang, X.; Wang, L.; Meier, H. Enhanced Performance of the Dye-Sensitized Solar Cells with Phenothiazine-Based Dyes Containing Double D–A Branches. *Org. Lett.* **2011,** *13*, 1610-1613.

(69)   De Angelis, F.; Tilocca, A.; Selloni, A. Time-Dependent DFT Study of [Fe(CN)6](4-) Sensitization of TiO$_2$ Nanoparticles. *J. Am. Chem Soc.* **2004,** *126*, 15024-15025.

(70)   Persson, P.; Bergstrom, R.; Lunell, S. Quantum Chemical Study of Photoinjection Processes in Dye-Sensitized TiO$_2$ Nanoparticles. *J. Phys. Chem. B* **2000,** *104*, 10348-10351.

(71)   Martsinovich, N.; Jones, D. R.; Troisi, A. Electronic Structure of TiO$_2$ Surfaces and Effect of Molecular Adsorbates Using Different DFT Implementations. *J. Phys. Chem. C* **2010,** *114*, 22659-22670.

(72)   Agrawal, S.; Dev, P.; English, N. J.; Thampi, K. R.; MacElroy, J. M. D. A TD-DFT Study of the Effects of Structural Variations on the Photochemistry of Polyene Dyes. *Chem. Sci.* **2012,** *3*, 416-424.

(73)   Cossi, M.; Rega, N.; Scalmani, G.; Barone, V. Structures, and Electronic Properties of Molecules in Solution with the C-PCM Solvation Model. *J. Comp. Chem.* **2003,** *24*, 669-681.

(74)   Frisch, M. J.; Trucks, G. W.; Schlegel, H. B.; Scuseria, G. E.; Robb, M. A.; Cheeseman, J. R.; Scalmani, G.; Barone, V.; Mennucci, B.; Petersson, G. A.*, et al. Gaussian 09*, Revision A.1; Gaussian, Inc.: Wallingford CT, 2009.

(75)   Pastore , M.; Fantacci, S.; De Angelis , F. Modeling Excited States and Alignment of Energy Levels in Dye-Sensitized Solar Cells: Successes, Failures, and Challenges. *J. Phys Chem. C* **2013,** *117*, 3685-3700.

(76)   Pastore, M.; Mosconi, E.; De Angelis, F.; Grätzel, M. A Computational Investigation of Organic Dyes for Dye-Sensitized Solar Cells: Benchmark, Strategies, and Open Issues. *J. Phys. Chem. C* **2010,** *114*, 7205-7212.

(77)   Agrawal, S.; Dev, P.; English, N. J.; Thampi, K. R.; MacElroy, J. M. D. First-Principles Study of the Excited-State Properties of Coumarin-Derived Dyes in Dye-Sensitized Solar Cells. *Journal of Materials Chemistry* **2011,** *21*, 11101-11108.

(78)   Dev, P.; Agrawal, S.; English, N. J. Determining the Appropriate Exchange-Correlation Functional for Time-Dependent Density Functional Theory Studies of Charge-Transfer Excitations in Organic Dyes. *The Journal of Chemical Physics* **2012,** *136*, 224301-11.

31

(79)   Yanai, T.; Tew, D. P.; Handy, N. C. A New Hybrid Exchange-Correlation Functional Using the Coulomb-Attenuating Method (CAM-B3LYP). *Chem. Phys. Lett.* **2004,** *393*, 51-57.

(80)   Kalyanasundaram, K.; Grätzel, M. Applications of Functionalized Transition Metal Complexes in Photonic and Optoelectronic Devices. *Coord. Chem. Rev.* **1998,** *177*, 347.

(81)   Falaras, P. Synergetic Effect of Carboxylic Acid Functional Groups and Fractal Surface Characteristics for Efficient Dye Sensitization of Titanium Oxide. *Sol. Energy Mater. Sol. Cells* **1998,** *53*, 163-175.

(82)   Finnie, K. S.; Bartlett, J. R.; Woolfrey, J. L. Vibrational Spectroscopic Study of the Coordination of (2,2′-Bipyridyl-4,4′-dicarboxylic acid)ruthenium(II) Complexes to the Surface of Nanocrystalline Titania. *Langmuir* **1998,** *14*, 2744-2749.

(83)   Srinivas, K.; Yesudas, K.; Bhanuprakash, K.; Rao, V. J.; Giribabu, L. A Combined Experimental and Computational Investigation of Anthracene Based Sensitizers for DSSC: Comparison of Cyanoacrylic and Malonic Acid Electron Withdrawing Groups Binding onto the TiO_2 Anatase (101) Surface. *J. Phys. Chem. C* **2009,** *113*, 20117–20126.

(84)   Ganbold, E.-O.; Lee, Y.; Lee, K.; Kwon, O.; Joo, S.-W. Interfacial Behavior of Benzoic Acid and Phenylphosphonic Acid on Nanocrystalline TiO_2 Surfaces. *Chem. Asian J.* **2010,** *5*, 852-858.

(85)   Nazeeruddin, M. K.; Humphry-Baker, R.; Liska, P.; Grätzel, M. Investigation of Sensitizer Adsorption and the Influence of Protons on Current and Voltage of a Dye-Sensitized Nanocrystalline TiO_2 Solar Cell. *J. Phys. Chem. B* **2003,** *107*, 8981-8987.

(86)   Lee, K. E.; Gomez, M. A.; Elouatik, S.; Demopoulos, G. P. Further Understanding of the Adsorption Mechanism of N719 Sensitizer on Anatase TiO_2 Films for DSSC Applications Using Vibrational Spectroscopy and Confocal Raman Imaging. *Langmuir* **2010,** *26*, 9575–9583.

(87)   Pérez León, C.; Kador, L.; Peng, B.; Thelakkat, M. Characterization of the Adsorption of Ru-bpy Dyes on Mesoporous TiO_2 Films with UV−Vis, Raman, and FTIR Spectroscopies. *J. Phys. Chem. B* **2006,** *110*, 8723-8730.

(88)   Pastore, M.; De Angelis, F. Computational Modelling of TiO_2 Surfaces Sensitized by Organic Dyes With Different Anchoring Groups: Adsorption modes, Electronic Structure and Implication for Electron Injection/Recombination *Phy. Chem. Chem. Phys.* **2012,** *14*, 920-928.

(89)   Anselmi, C.; Mosconi, E.; Pastore, M.; Ronca, E.; De Angelis, F. Adsorption of Organic Dyes on TiO_2 Surfaces in Dye-Sensitized Solar Cells: Interplay of Theory and Experiment. *Phy. Chem. Chem. Phys.* **2012,** *14*, 15963-15974.

(90)   Weng, Y.-X.; Wang, Y.-Q.; Asbury, J. B.; Ghosh, H. N.; Lian, T. Back Electron Transfer from TiO_2 Nanoparticles to FeIII(CN)$_6$$^{3-}$:□ Origin of Non-Single-Exponential and Particle Size Independent Dynamics. *J. Phys Chem. B* **2000,** *104*, 93-104.

(91)   Khoudiakov, M.; Parise, A. R.; Brunschwig, B. S. Interfacial Electron Transfer in FeII(CN)64-−Sensitized TiO_2 Nanoparticles:□ A Study of Direct Charge Injection by Electroabsorption Spectroscopy. *J. Am. Chem Soc.* **2003,** *125*, 4637-4642.

(92)   Pastore, M.; De Angelis, F. Intermolecular Interactions in Dye-Sensitized Solar Cells: A Computational Modeling Perspective. *J. Phys. Chem. Lett.* **2013**, 956-974.

32